

# Optical Tau in Boundary-Avoidance Tracking - A New Perspective on Pilot-Induced Oscillations

Linghai Lu\*, Gareth D. Padfield, and Michael Jump  
*Flight Science & Technology, School of Engineering*  
*University of Liverpool, Liverpool, L69 3GH, UK*  
 \*Email: [Linghai@liv.ac.uk](mailto:Linghai@liv.ac.uk)

Tau theory, recently introduced to the flight control discipline as a model for natural guidance, is shown to provide an alternative approach to predicting a class of adverse aircraft-pilot couplings described as boundary-avoidance tracking (BAT) events and PIOs. These have previously been modelled as discrete events developed using time dependent feedback gains. Drawing on the prospective nature of the time-to-contact variable, optical tau, a new method is proposed for modelling such phenomenon, and also determining the critical incipience for this class of event and PIOs. In the present study, the approach has been used to demonstrate tau guidance in a rotorcraft trajectory tracking manoeuvre and to predict the conditions under which a BAT event or BAT PIO may occur. In addition, a strong correlation between motion and control activity and the derivatives of tau adds substance to the hypothesis that the pilot's perceptual system works directly with optical variables during visual guidance. Results from flight simulation tests conducted at The University of Liverpool, and complementary flight tests carried out with The National Research Council (Canada) ASRA in-flight simulator, support the tau control hypothesis. The theory suggests ways that pilots could be alerted to the impending threat of such adverse aircraft-pilot couplings.

## Nomenclature

$a$	= acceleration, ft/s <sup>2</sup>
$g$	= acceleration due to gravity, ft/s <sup>2</sup>
$h$	= height above terrain, ft
$k$	= coupling constant
$K, K_m$	= boundary tracking feedback gain and its maximum value
$t$	= time, s
$t_{\max}$	= time point when the pilot responds to the boundary with maximum input, s
$t_{\min}$	= time point when the pilot first responds to the boundary, s
$T$	= duration of a manoeuvre, s
$v$	= velocity, ft/s
$V_x, V_y$	= forward and lateral speed, kts
$x, \dot{x}$	= distance to and closure rate along the runway, ft, ft/s
$x_d$	= lateral cyclic control input (pilot stick), in
$x_g$	= intrinsic tau guidance gap profile, ft
$y, \dot{y}$	= distance to and closure rate across the runway, ft, ft/s
$\theta_{lc}$	= lateral control input angle, deg
$\tau$	= optical tau, the instantaneous time to contact boundary in the optical field, s
$\dot{\tau}, \ddot{\tau}$	= rate and acceleration change of optical tau
$\tau_d$	= system time delay, s
$\tau_{\max}$	= time-to-boundary when applying maximum input, s
$\tau_s$	= timing of initiating the deceleration phase, s
$\tau_x, \tau_y$	= motion tau in the $x$ and $y$ direction in the runway reference system, s, s

## Subscripts

0	= initial values
---	------------------

$b$	= boundary
$b_e, b_s$	= start and end of boundary avoidance
$bsw$	= start of boundary avoidance from Warren's method
$e$	= edge of the runway or $\pm 70$ ft line
$g$	= intrinsic tau guidance
$i$	= iteration number

## Symbol

$\wedge$	= Normalised terms
----------	--------------------

## I. INTRODUCTION

The traditional view of how pilots perform a wide range of flying tasks involves an initial acquisition, followed by point tracking (PT) of aircraft flight path or attitude. Having acquired the desired flight path or vehicle attitude, the pilot tries to maintain this at some fixed value. One category of Pilot Induced Oscillations (PIOs) results from the pilot increasing gain during the tracking phase [1-4]. Situations when pilots might operate aircraft within attitude and flight-path constraints, using high feedback gain, include air-to-air refuelling, formation flying and target tracking, or operations in confined areas. Gray proposed a piloting strategy to explain a class of PIOs that can occur termed Boundary Avoidance Tracking (BAT) [5]. He noted that there are times when pilots deviate from classical PT behaviour and instead, adopt a strategy that requires them to monitor and avoid one or more boundaries (e.g. such as when trying to avoid ground impact while, at the same time, preventing low altitude departure from controlled flight). PIOs may also occur under these situations and are distinct from classical PT PIOs in that they are triggered by the pilot needing to manage the aircraft approaching potentially opposing boundaries. Current understanding and knowledge about PIOs are considered inadequate to explain these BAT control strategies.

A new pilot model, based on boundary-avoidance feedback as a function of the instantaneous time to the boundary in question, has been proposed by Gray. It is characterized by three parameters - the time at which a pilot is first aware of the existence of the boundary and takes action ( $t_{\min}$ ), the time corresponding to the maximum control deflection ( $t_{\max}$ ) and the maximum BAT feedback gain ( $K_m$ ). In Gray's work, these parameters were initially found through trial and error, then later using an optimization approach that minimized the difference between the predicted control inputs and those recorded in flight/simulation.

Based on Gray's initial work, Warren proposed an analytic approach to determine the values of  $t_{\min}$ ,  $t_{\max}$ , and  $K_m$  and their relationship to open-loop characteristics such as system time delay and crossover frequency [6;7]. Among these parameters,  $t_{\min}$  was originally considered to be the most difficult to identify, and Warren proposed that it could be determined by the first sharp increase in the control force/acceleration to prevent exceeding the impending boundary. Warren [7] successfully applied this new approach to analyse flight test data. However, the task of relating control movement to boundary stimuli by visual inspection of the data was complicated by coupling between the frequent control inputs and the ensuing vehicle dynamics response. Pavel et al. [8] examined this model for helicopter pitch tracking tasks and predicted the (spatial) point in the manoeuvre when the pilot switched between PT and BAT strategies.

The work of Gray and Warren is fundamentally based upon the pilot's perception of the time-to-contact, or tau, introduced by Lee [9] as a development of Gibson's optical flow theory of visual perception [10]. The development of tau theory is based on the premise that purposeful actions are accomplished through coupling the motion with either external or internal sources - the so-called motion guides [9;11-13]. Motivated by its basis in visual perception, tau has been applied to flight control and handling qualities [1;14-17], with the hypothesis that, in terms of a visual guidance strategy, the overall pilot's goal is to overlay the perceived optical flow-field over the required flight trajectory; the pilot then works directly with optical variables to achieve prospective control of the aircraft's future trajectory. One of the first reported applications of tau-coupling to aircraft flight [14] considered tau-guidance control strategies during a helicopter stopping manoeuvre close to the ground. An investigation of terrain-hugging flight reinforced the prospective control behaviour of helicopter pilots [1;15;18]. In addition, similar results have been found by application to the landing flare manoeuvre of fixed-wing aircraft [16;17].

The present paper extends the application of tau theory to boundary avoidance tracking using a 'roll-step' manoeuvre [19], developed to evaluate lateral-directional handling qualities of rotorcraft, as an extension of the ADS-33 mission task element family [20]. Because of the close relationship between the BAT concept and tau theory, an objective of the research is to use tau theory to detect a BAT event by determining  $t_{\min}$  and associated BAT timings, and furthermore to establish if tau theory provided clues to the incipience of a PIO. A more general objective is to explore how the pilot's perception system works directly with the available optical

information, thus establishing a relationship between the aircraft motion, control activity and the optical flow variables in a new model of BAT PIOs.

The paper begins with a summary of the BAT model. The roll-step manoeuvre is described and tau theory introduced and used to model the control strategy through tau guidance and hence to determine the BAT model parameters for comparison with Gray's method. Rules for establishing the likelihood of BAT events are proposed.

## II. REVIEW OF BAT THEORY

### A. Introduction of the BAT model

Although the available literature and research findings related to the modelling of pilot behaviour is extensive [1;21], it remains difficult to predict aspects of pilot control activity, particularly during incipient PIOs. The BAT theory, introduced by Gray [5], suggests that this deficiency originates from the assumption that a pilot will always attempt to maintain a key parameter at some single value - the point tracking strategy. However, based on anecdotal evidence from pilots [5], this assumption can be violated in practice in that the pilot may actually focus on avoidance of, or limiting closure to, operationally imposed boundaries.

Gray developed the BAT model, shown in Fig. 1, and provided analysis techniques for predicting the associated boundary-avoidance model parameters.

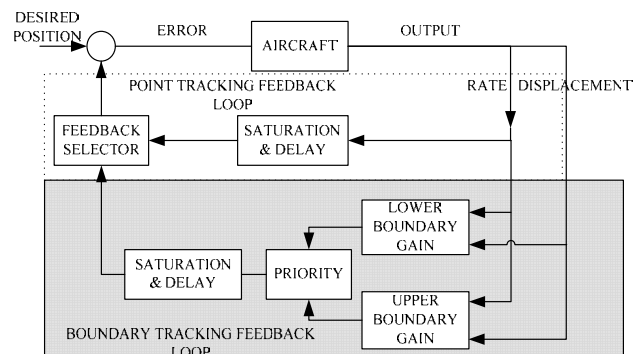


Fig. 1 The boundary-avoidance tracking model (based on [5])

The feedback loop includes both point and boundary tracking options with a logic switch/selector that assumes no transient; only one of the tracking channels is assumed to take place at any one time. There are two boundaries in this particular model, designated upper and lower, and, crucially, only one can be tracked at a time, depending on its priority.

A key parameter in the BAT model is the time to boundary ( $\tau_b$ ), based on the displacement to boundary ( $x_b$ ) at the current approaching rate ( $\dot{x}_b$ ), defined as follows:

$$\tau_b = \frac{x_b}{\dot{x}_b} \quad (1)$$

The switching between PT and BAT and the variation of the BAT feedback gain  $K$  are illustrated in Fig. 2. The overall gain

$K$  models the control deflection in a ramp-attenuated, bang-bang, form.

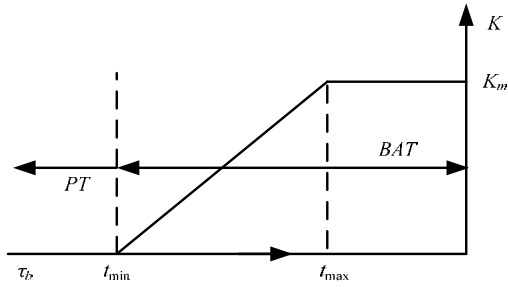


Fig. 2 Feedback gain variation with the time to boundary ( $\tau_b$ ) [5]

The BAT strategy is initiated when  $\tau_b$  is less than the value  $t_{\min}$  (minimum control efforts). If the boundary continues to be approached, the feedback gain increases linearly to its maximum,  $K_m$ , in the form;

$$K = \frac{t_{\min} - \tau_b}{t_{\max} - t_{\min}} K_m \quad (2)$$

The feedback gain and control input are kept at this maximum level when  $\tau_b$  is less than the value  $t_{\max}$  (maximum control effort). If the boundary is exceeded, the BAT model gain remains at its maximum level. The BAT model strategy is thus based on a ramp-type bang-bang control, with ramp slope a function of the instantaneous time to the boundary.

To use the BAT model of pilot behaviour, the three BAT parameters ( $t_{\min}$ ,  $t_{\max}$ , and  $K_m$ ) need to be found.  $t_{\min}$  is determined by detecting the change of the control acceleration as discussed.  $t_{\max}$  can be computed at the time-to-boundary point when the maximum control deflection occurs. Finally, the value of  $K_m$  is the amplitude of the maximum control input applied.

Using Eq. (2), Gray and Warren hypothesized that the control increases linearly as the boundary is approached. They recognized that this process is likely to be non-linear in practice, influenced by the complexity of the pilot's prospective control, the channels used to sense information, the flight control system and the aircraft aerodynamic characteristics. Moreover, the pilot may not always apply the maximum input for different BAT events, except perhaps when reaching control saturation. When the pilot perceives that the hazard posed by the impending boundary is reducing, the control input will gradually be reduced to avoid other problems, such as reaching rate limits. Therefore, in reality, both  $t_{\max}$  and  $K_m$  are likely to be 'adaptive' parameters.

Warren estimated the parameter  $t_{\min}$  using the control acceleration, computed by numerically differentiating the control deflection. However, this method is not straightforward because there are many control movements that do not serve the tracking objective. Warren also noted the failure of the direct determination of  $t_{\min}$  from the raw flight test data recordings due to sensor noise [7]. Therefore, to obtain sufficiently smooth data, a filtering process was necessary. This can reduce the useful information contained in

the raw data and lead to lower levels of confidence in the predicted value of  $t_{\min}$ . As a consequence, in addition to investigating the nonlinearities integral to the BAT model, and its characteristic parameters, one of the objectives of this paper is to provide a methodology to predict the occurrence of a BAT event. Once such an event is in progress, a question is - are there unique control patterns that might be used to trigger warning systems; this is another theme of the paper.

### III. DESCRIPTION OF THE ROLL-STEP MISSION TASK ELEMENT

The roll-step mission task element (MTE) was selected because it exposes the pilot-aircraft system to potentially adverse PIOs during tight flight-path tracking. Both ground based simulation and flight test data were available from tests conducted on The University of Liverpool's flight simulators [22;23] and the Bell 412 ASRA of the Canadian National Research Council (NRC). The simulation model used was the nonlinear FLIGHTLAB Bell 412 - F-B412[24].

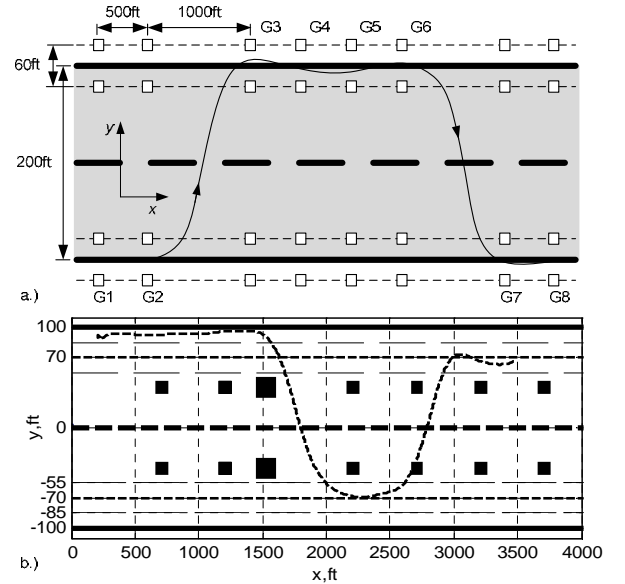


Fig. 3 Layout of roll-step test MTEs

The roll-step shown in the two versions used in Fig. 3 is a Handling Qualities (HQ) MTE [19;20]. The helicopter is initially flown along the runway edge. In the upper figure, upon reaching the gate (G2), the pilot initiates a turn, manoeuvring the aircraft to fly through the gate (G3), located on the other side of the runway. The pilot then guides the aircraft along the runway edge and passes through several gates (G3 to G6), before initiating a second runway crossing manoeuvre, to fly through (G7). The inner and outer gate posts represent the adequate boundaries in HQ parlance - the boundaries of acceptable performance and safety ( $\pm 30$  ft); the desired performance is set at 50% of this value ( $\pm 15$  ft). The lower figure shows the layout for the flight test at Ottawa International airport, where the markings are more sparse. For the flight and related simulation cases, the pilots were required

**Table 1 Configurations used for simulation and flight experiments**

Cases	Simulator (Sim)									Flight test (FT)			
	SA 1	SA 2	SA 3-5	SA 6-7	SA 8	SA 9	SA 10-11	SA 12-13	SA 14-17	FR 1	FR 2	FA 1	FA 2
$V$ , knots	40	80	80	80	100	100	100	60	60		26	36	30
$h$ , ft	10	10	20	40	10	20	40	45	45	45	45	65	65
ACAH	off	off	off	off	off	off	off	on	off	on	off	on	off
Motion	off	on	on	on	on	on	on	on	on	--	--	--	--

to initiate the manoeuvre from the dashed line (+70 ft) and then to line up with the dashed line (-70 ft) located at the other side of the runway. No adequate performance boundary markings were present at the airfield, so the pilots were asked to stay within an imaginary track ( $\pm 15, \pm 30$  ft) either side of the dashed lines. The level of aggressiveness required to accomplish the manoeuvre depends on the flight speed on the one hand and the aircraft performance and agility on the other; for example, at 60 kts flight speed, the time to pass from gate G2 to G3 is about 10 seconds; at 100 kts, the time reduces to 6 seconds. As speed increases and aircraft roll agility (e.g. attitude quickness) reduces, the risk of task failure and the propensity for roll PIOs during the runway edge acquisition and subsequent tracking increases.

**B. Motion gaps and key elements in the roll-step MTE**

In this paper, only results from the first half of the MTE (from G2 to G3 and on to G6 in Fig. 3) are presented because of the approximate symmetry from G6 to G8 and beyond. The roll-step consists of a lateral acceleration-deceleration where a bank angle is applied at G2 to initiate the lateral acceleration, followed by a roll reversal and deceleration phase. The primary control is the lateral cyclic. With an over-aggressive initiation at G2 or late commencement of the deceleration phase, a BAT PIO can occur as the gate at the runway edge is approached. Higher speeds will demand a more aggressive control strategy – a higher required bank angle, more rapid control action etc. - hence the propensity to PIO will increase. Throughout the roll-step, the pilot needs to close a number of motion gaps synchronously and sequentially with rapidly coordinated actions – bank angle, heading etc. For example, to reach the gate at G3 requires synchronous closure of the  $x$  (along runway) and  $y$  (cross-runway) motion gaps.

If the pilot initiates the deceleration late, the focus of attention can change from the runway edge to the adequate performance boundary at the outer gate post of G3. The narrower the adequate corridor, the greater the risk that the pilot will have insufficient time to manoeuvre within the boundaries, switching from one side to the other. In such circumstances, continued attempts to fly the task may result in a PIO. Apart from these motion-gap closures, the pilot is also required to maintain speed and height constraints to accomplish the manoeuvre. All these can contribute to an increase in the pilot’s workload, resulting in lateral control inputs being delayed or flawed as a result of divided attention.

The experimental configurations used for the simulation and flight tests are listed in Table 1.  $V$  and  $h$  are the initial flight

velocity and height above ground respectively. Table 1 contains twenty-one experimental test cases in total. The first seventeen cases were flown in the simulator, prefixed SA. Among these, SA1-11 were conducted with the height and speed constrained at the initial conditions of the simulation. The other six cases (SA12-17) had no such constraints. The four cases prefixed F are from the flight test and, obviously, have no constraints. For the cases without constraints, the height was selected by the pilots during the run-in to the roll-step and this was to be maintained during the MTE. In addition, two pilots (A and R) were involved in the flight experiments, although only one of these flew the ground-based simulation tests (A). Moreover, five cases (three simulator tests and two flight tests) were flown with an attitude command, attitude hold control system engaged (ACAH-on, providing nominally Level 1 handling qualities); all other cases were flown with the (nominally Level 2) bare airframe configuration.

As a pre-cursor to the summary of tau theory, Fig. 4 illustrates the instantaneous time to the runway edge,  $\tau_e = y(t)/\dot{y}(t)$ , as a function of normalised manoeuvre time (where  $y(t)$  is the distance to the runway edge) for several flight and simulation runs. In some cases, there is an apparent linear tendency in the second-half half of the motion, suggesting a constant rate of change of  $\tau_e$ . In others,  $\tau_e$  appears to level off before diverging with a negative  $\dot{\tau}_e$  the aircraft never reaching the edge in these cases.

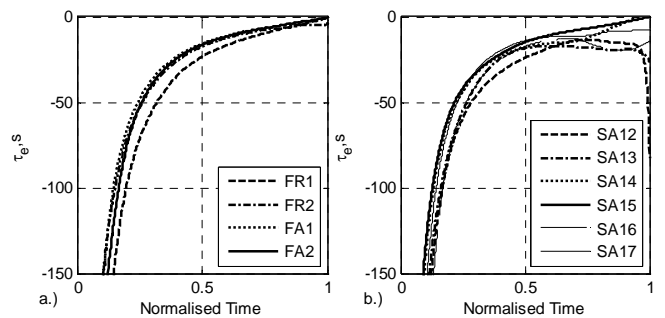


**Fig. 4 Motion tau of the roll-step manoeuvre as a function of normalised time**

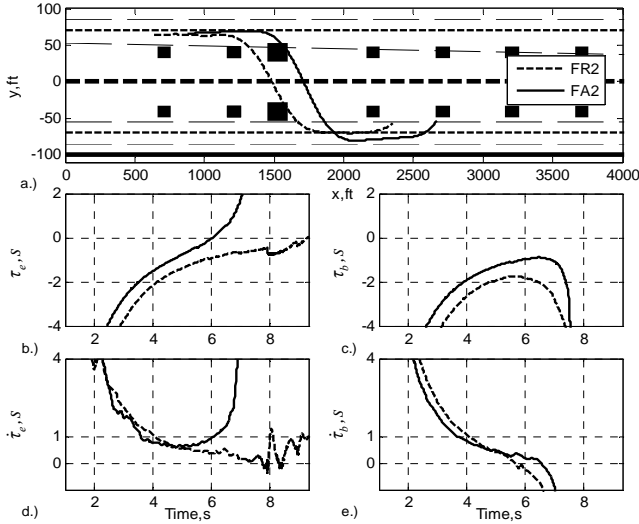


**Fig. 5 Illustration of two typical kinds of roll-step manoeuvres**  
FR2: no BAT event, FA2: possible BAT event

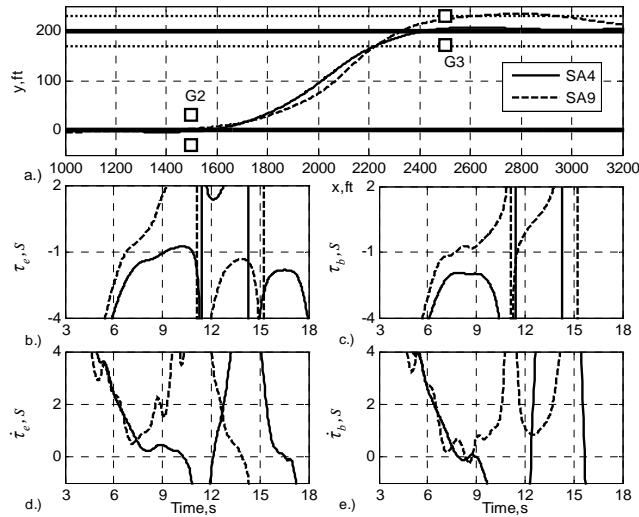


**Fig. 6 Illustration of  $\tau$  variations in typical roll-step manoeuvres**

To understand these patterns better, four typical cases SA4, SA9, FR2 and FA2 are shown in Fig. 5 and Fig. 6. In FR2, the pilot closes the gap smoothly as  $\tau_e$  approaches zero with a  $\dot{\tau}_e$  of about 0.5, lining up with the runway edge with no overshoot. The time to the outer adequate boundary,  $\tau_b$ , reduces to about 2 seconds before diverging again as the pilot lines up with the runway. In run FA2, the pilot overshoots the edge at  $t = 6$  seconds, from an approach with  $\dot{\tau}_e > 0.5$ , coming within one second of the adequate boundary. In SA4,  $\dot{\tau}$  settles to a constant low value prior to the edge crossing, followed by a series of crossings as the pilot tracks the edge. SA9 shows the pilot overshooting both the runway edge and the outer adequate boundary (at 10 seconds). From there, the pilot flies inside the adequate boundary again at about 12 seconds and never manages to align with the runway edge during the manoeuvre shown ( $\tau_e \leq -2$  seconds). The spikes in the traces occur when the velocity passes through zero.

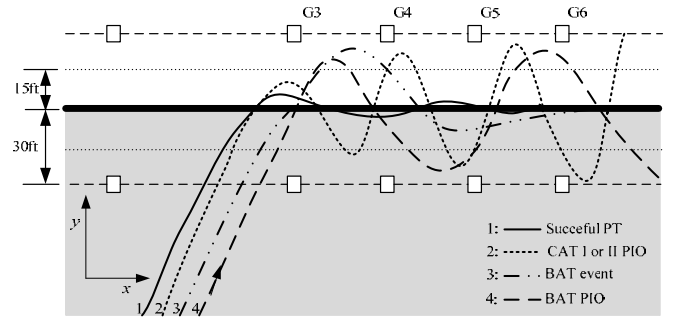


**Fig. 7 Different scenarios during a tracking task**

As a pilot approaches a tracking task, it is hypothesised that four possible scenarios can develop, illustrated in Fig. 7. A successful tracking is shown as case 1, with the flight trajectory aligning smoothly with the runway edge. The pilot's focus of attention is the runway edge tracking and there appears to be no disruption from the proximity of the outer boundaries. A classic CAT II PIO [1;4] is shown as case 2, where the pilot struggles with the tracking, driving the combined pilot-aircraft unstable and the flight path oscillations diverge. When the control inputs are so aggressive that the actuators saturate, case 2 can develop into a CAT II PIO. Case 3 is the BAT event, where the pilot overshoots the runway edge and switches attention to the outer boundary. The pilot successfully avoids crossing the boundary and switches attention back to successfully tracking the runway edge; this situation is described as a BAT event since the pilot switched from point to boundary avoidance tracking. In the 4<sup>th</sup> case, the pilot fails to re-establish point tracking and, instead, the manoeuvre develops into a BAT PIO between the adequate performance boundaries. In the results from the trial series drawn on for this paper, examples of the first three cases described above will be shown. Classification of the four cases in terms of  $\tau$  and its derivatives at the runway crossing point will be developed.

## IV. RÉSUMÉ OF TAU THEORY

### A. Optical tau ( $\tau$ ) –perceptual and prospective guidance

The BAT model is fundamentally based on the perceived time-to-edge ( $\tau_e$ ) and time-to-boundary ( $\tau_b$ ) in Eq. (1) with the BAT control gain a function of  $\tau_b$ . The time to edge/boundary is equivalent to the temporal time-to-contact variable tau ( $\tau$ ) for closure of a gap in the optical field,

$$\tau(y, t) = \frac{y}{\dot{y}} \quad (3)$$

where  $y$  is the motion gap and  $\dot{y}$  is the gap closure rate. The term ‘motion gap’ refers to a perceived difference between the observer's current and desired target state/position. The concept of a motion gap was formulated by Lee [9] when developing general  $\tau$ -theory; Lee modelled how organisms control their movement prospectively through the cluttered environment close to the Earth's surface. Lee also postulated

that a motion gap was not necessarily limited to an observable physical distance, but could also take other forms such as force (e.g. when taking a step whilst walking), hearing (e.g. whilst playing an instrument), and pitch (e.g. when singing a song), etc. [12]. Moreover, tau theory provides the attractive proposition that the *tau of a motion variable* can be sensed directly by subjects, i.e. quantifying the size of the motion gap and its approach velocity is not required for the motion to be perceived and controlled. A number of examples offer evidence to support this point [9;11-13;15], and that this is the result of natural evolutionary processes – that movement guidance should be simple, rapid, reliable and biologically plausible – otherwise, the guidance may be degraded by associated delays and noise contamination [9;12;13].

In this paper, the distance to the runway edge and to the adequate performance boundary are treated as the spatial gaps, controlled by sensing and constantly adjusting the  $\tau$  variable, regardless of the approach velocity and acceleration of the aircraft. To avoid the boundary, the pilot has to predict the flight path sufficiently far ahead to apply prospective control. This hypothesis therefore constructs a bridge between the BAT and tau theories.

### B. Tau-coupling guidance

In practice, there are often two or more gaps needed to be closed simultaneously, such as the coordination required between the lateral and forward motions, or forward and vertical motions, in order to achieve a combined horizontal-vertical manoeuvre [19]. Two motions  $[x(t)$  and  $y(t)]$  are said to be tau-coupled if the following relationship is satisfied,

$$\tau_y = k\tau_x \quad (4)$$

The coupling term  $k$  in Eq. (4) regulates the dynamics of the motions in the  $x$  and  $y$  directions. The detailed derivation of the motion laws are given in Appendices A and B. By keeping the tau's of motion gaps in a constant ratio, tau - coupling results in effective movement coordination through a power law (for  $x < 0$ ),

$$y = C(-x)^{1/k} \quad (5)$$

The tau-coupled motion gaps can be of two forms – extrinsic motion-gaps ( $x$  and  $y$  are physically observable) and intrinsic, sensory, motion gaps ( $y$  is physically observable while  $x$  is internally generated by the perception system). The intrinsic motion gaps are assumed to be generated by internal sensory arrays [13], required when extrinsic variables are not available to guide movement, such as self-paced movement in which only one motion-gap is involved [12]. In this case, intrinsic guidance of movement (through a so-called tau-guide,  $\tau_g$ ) is hypothesized to be modelled through the following relationship:

$$\tau_y = k\tau_g \quad (6)$$

The  $\tau_g$  guidance is based upon the premise that an internally generated motion guide provides the stimulus onto which an externally perceived gap can be coupled. It can be shown that

for general deceleration-to-stop-motions, the natural intrinsic guide can take the form of either a constant velocity or a constant deceleration [1;13] where,

$$\text{for constant velocity guidance} \quad \hat{\tau}_g = -(1-\hat{t}) \quad (7)$$

$$\text{for constant deceleration guidance} \quad \hat{\tau}_g = -\frac{1}{2}(1-\hat{t}) \quad (8)$$

The dressing ‘ $\hat{\phantom{x}}$ ’ indicates that the related terms are normalised by  $T$ , the duration of the manoeuvre, so that  $0 < \hat{t} \leq 1$ . These forms of coupling both result in a motion where the rate of change of  $\tau_y$  with time is constant,

$$\text{for constant velocity guidance} \quad \dot{\tau}_y = k \quad (9)$$

$$\text{for constant deceleration guidance} \quad \dot{\tau}_y = \frac{k}{2} \quad (10)$$

More general, point-to-point motions (e.g. hover to hover) can be accomplished by following the constant acceleration guide [1]; the motion equations are also derived in Appendix A for completeness. The significance of the constant acceleration or deceleration guides is suggested to stem from the influence of gravity on humans’ and animals’ movement during the period of evolution, [9;12], while constant velocity is mimicked by horizontal motions of thrown objects, at least in the short term. Experiments have verified the existence of the intrinsic tau information embodied in the nervous system [12], as well as the presence of  $\tau_g$  guidance in aircraft operations [14-17].

### C. Control strategy in the deceleration/capture phase of the roll-step MTE

To avoid the hazard of an impending boundary a pilot has to fly a continuous deceleration manoeuvre to control the motion gap to the boundary. The hypothesis is that the only information the driver/pilot needs is the rate of change of tau with time,

$$\dot{\tau}_y = 1 - \frac{y\ddot{y}}{\dot{y}^2} = 1 - \frac{\tau_y}{\tau_y} \quad (11)$$

For the special case of a one-dimensional deceleration it can be seen that tau-coupling between the distance to go and its time derivative i.e.  $\tau_y = (1 - \dot{\tau}_y)\tau_y$ , is equivalent to a  $\dot{\tau}$  constant motion. Research into vehicle stopping normally involves one deceleration goal, while the BAT event/PIO involves a series of continuous collision-avoidance manoeuvres. However, with the hypothesis that only one event happens at one time, the whole BAT process can be analyzed contiguously with the idea that the switching strategy leads to a conflict of control and the potential of a PIO.

A  $\dot{\tau}$  constant motion can therefore be modelled as either an intrinsic tau-guide following strategy, where the guide takes the form of a constant deceleration (or velocity), or with an extrinsic guide, the pilot coupling the motion and its velocity. With the situation that  $y < 0$  and  $\dot{y} > 0$ , the five situations shown in Table 2 are possible for such motion-gap closures [12;15;25]. Typical cases are illustrated in Fig. 8 in normalised form (time is normalised by the manoeuvre time).

**Table 2 Aircraft kinematics with different  $\dot{\tau}$  values; following a constant deceleration guide**

No.	$\dot{\tau}$ Values	$k$	Aircraft Dynamic Status
1	$\dot{\tau} > 1$	$k > 2$	Accelerating flight towards the goal/boundary
2	$\dot{\tau} = 1$	$k = 2$	Constant-velocity flight towards the goal/boundary
3	$0.5 < \dot{\tau} < 1$	$1 < k < 2$	Decelerating flight with infinite deceleration at boundary
4	$\dot{\tau} = 0.5$	$k = 1$	Constant decelerating flight stopping at the boundary
5	$0 < \dot{\tau} < 0.5$	$0 < k < 1$	Decelerating flight with maximum finite deceleration earlier in manoeuvre as $k$ reduces

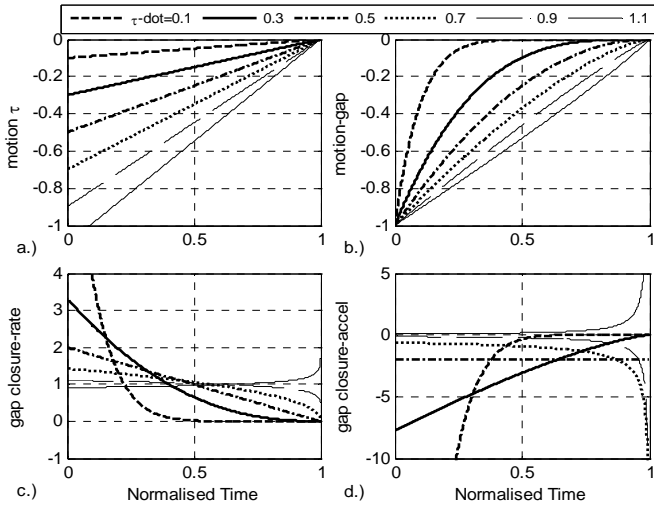


**Fig. 8 Kinematics of motion following a constant deceleration guide in normalised form (Appendix A)**

Stopping at the goal is therefore possible with a finite deceleration provided  $k \leq 1$  ( $\dot{\tau} < 0.5$ ). Fig. 8 and the expressions in Appendix A show that for these cases the motion also has a finite initial deceleration, increasing with decreasing  $k$ .

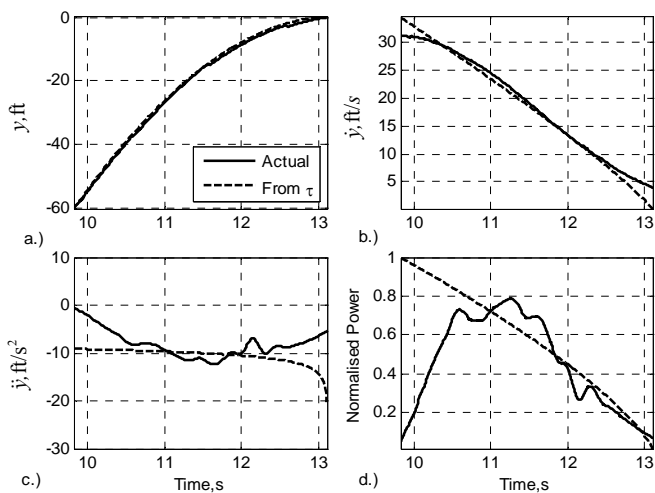


**Fig. 9 Comparison of actual motion with the 'best fit' guide following motion for flight case FR2,  $k \approx 1.0$**

In addition, a particular motion corresponds to the case when  $k = 1$ , with a constant deceleration throughout the approach. Fig.

9 shows a comparison of the distance to the runway edge, velocity and deceleration for FR2, for the 3 seconds of the 'near-perfect' constant decelerating approach. The actual trajectory matches the guide following trajectory very closely. Also shown in Fig. 9 is the variation of the normalised power (proportional to  $y\ddot{y}$ ) showing the nearly linear release of the kinetic energy of the aircraft during the deceleration to the runway edge.

Previous investigations have shown that humans and animals tend to adopt such constant  $\dot{\tau}$  strategies during the deceleration phase for visually guided movements, such as a hummingbird docking on a feeder tube [13], automobile braking [25], helicopter quick-stop manoeuvres (where  $\dot{\tau} \approx 0.5$  was common [14]), and during the flare manoeuvre in a fixed-wing aircraft [16;17]. Before applying tau guidance during the roll-step manoeuvre will be further discussed, with particular examination of the  $\dot{\tau}$  constant hypothesis for the deceleration phase.

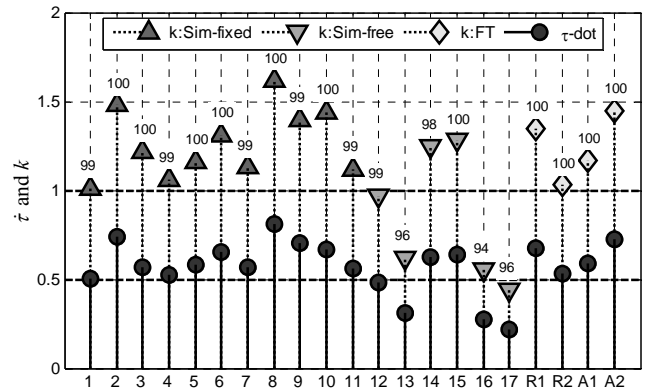


**Fig. 10  $\dot{\tau}$  and  $k$  values for aircraft motion and constant deceleration guide in the deceleration phase (the superscript numbers are %  $R^2$  values during deceleration)**

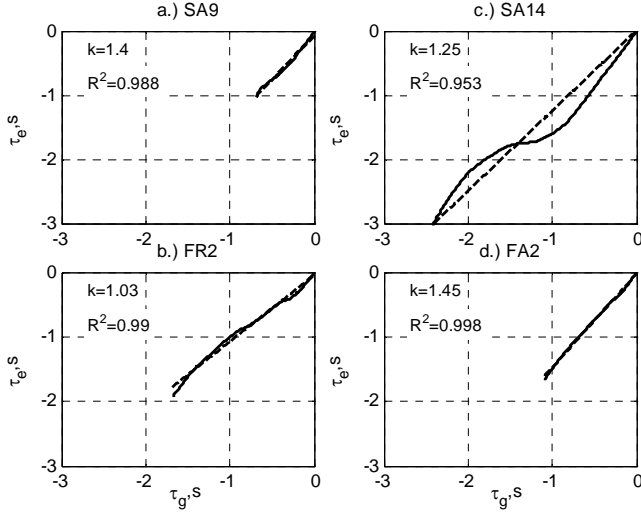


**Fig. 11 Correlation of  $\tau_e$  for aircraft motion and constant deceleration guide for four cases in the deceleration phase – simulation test ( $\dot{\tau} = k/2$ )**

Fig. 10 and Fig. 11 show the close fit with the constant deceleration guide in the deceleration phase of the roll step for a number of simulation and flight runs. The cases with  $k$  values  $> 1$  imply hard decelerations to the runway edge (as suggested in Table 2), often with runway crossings, while others with  $k < 1$  being soft decelerations, where the maximum lateral deceleration occurs early in the MTE.

In summary, for an aircraft initially accelerating towards a goal  $\dot{\tau} > 1$ , the deceleration phase commences when  $\dot{\tau} = 1$ , and if the pilot follows the constant deceleration guide to the goal, he will settle at the selected value of  $\dot{\tau}$ . At this crucial point, the manoeuvre time is determined by the initial  $\tau(\dot{\tau} = 1)$ , and the selected  $\dot{\tau}$  (see Appendix A), i.e.

$$T = -\frac{\tau_y(0)}{\dot{\tau}_y} \quad (12)$$

It is suggested that  $\tau_y(0)$  is the trigger here, the pilot selecting the deceleration profile depending on the urgency of the situation and the manoeuvre performance capability. The  $\dot{\tau}$  constant strategy has implications for the control usage throughout the manoeuvre and, although this depends on the response type of the aircraft, it can be shown that there is a strong correlation between control and variations in  $\dot{\tau}$ , hence the higher order derivative  $\ddot{\tau}$  takes its place in tau guidance and in the prediction of BAT event and PIO incipience.

## V. DETERMINATION OF BAT PARAMETERS BY OPTICAL TAU

The trajectory of a typical roll-step manoeuvre featuring a BAT PIO is illustrated in Fig. 12. The case is hypothetical as there were no fully developed BAT PIOs in the test data.

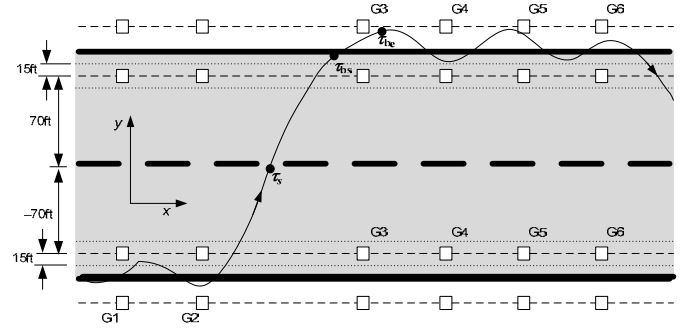


**Fig. 12 Illustration of BAT PIO in the roll-step manoeuvre**

The tracks joining the gate posts are the adequate performance boundaries. In Gray's model, three variables,  $\tau_s$ ,  $\tau_{bs}$ , and  $\tau_{be}$ , that describe the BAT are shown.  $\tau_s$  is the time that the pilot initiates the deceleration phase of the roll step. The variables  $\tau_{bs}$  and  $\tau_{be}$  are the times to boundary at the start and end timing points of the BAT (at  $t_{min}$  and  $t_{max}$  from Fig. 2). In the following Section, an approach based on the tau theory will be developed to provide answers to the questions raised earlier in the paper – when does the BAT event/PIO commence ( $\tau_{bs}$ ), when does it end ( $\tau_{be}$ ) and, crucially, can we predict the PIO ahead of its actual occurrence?

### A. Determination of $\tau_s$

The deceleration phase needs to be initiated at an appropriate moment to successfully achieve the roll-step manoeuvre. If the turn is initiated too early, or too late, additional pilot workload will be required to correct the flight path in a subsequent part of the manoeuvre. The timing depends on a number of factors, such as a pilot's experience and aircraft performance, but principally on the pilot's ability to perceive critical visual information. The tau of the motion-gap can govern this timing. For example, research into terrain following flight has shown that the pilot relies on motion perception about 6-8 seconds ahead [14], then taking action 2-3 seconds ahead, and this forms a foundation for the following analysis.

As the boundary is approached, when  $\dot{\tau}_e$  to the runway edge = 1, the closure of the motion gap transitions from acceleration to deceleration (Table 2). This critical moment is an effective indicator of control strategy and can thus be detected through the variations in both  $\dot{\tau}_e$  and  $\ddot{\tau}_e$ . The case FR2 is presented for illustration in Fig. 13.

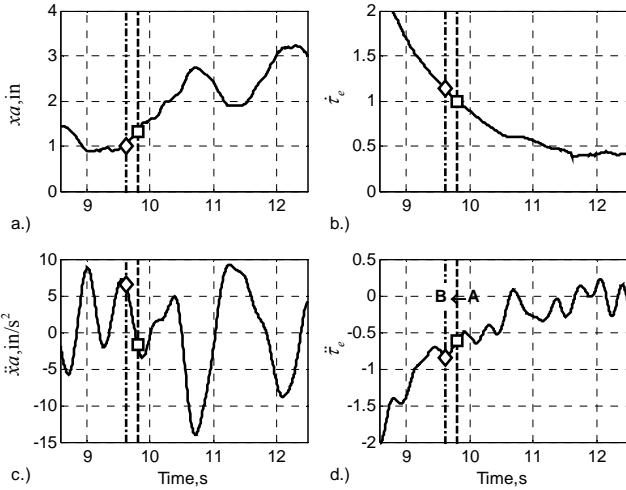


Fig. 13 Determination of  $\tau_s$  (case FR2)

Firstly, the  $\tau_s$  value for  $\dot{t}_e = 1$  is computed in Fig. 13b (square symbol). Attention is then turned to the corresponding point in the  $\ddot{t}_e$  curve. If the related point is located on a peak in the  $\ddot{t}_e$  data, then this is the desired  $\tau_s$  value. Otherwise, the closest following peak is chosen as shown in Fig. 13c (diamond symbol, A to B), corresponding to the peak in the acceleration of the control movement, the defining point for  $\tau_s$  in Gray's model.

Although Warren [6] suggested that the stick acceleration be a direct indicator of pilot strategy, the connection is not so apparent in Fig. 13a. Although the peak in  $\ddot{t}_e$  corresponds with a peak in the control acceleration, whether or not this particular sharp movement corresponds to the initiation of the deceleration is unclear. The identification problem is compounded by the need to differentiate the recorded control signal twice, a process requiring additional filtering and smoothing. Useful information within the data may be lost and a time delay introduced by these processes, affecting the computation of  $\tau_s$ . Moreover, even with perfect control acceleration information, it is still not possible to determine  $\tau_s$  uniquely because of the difficulty of determining exactly which sharp increase is the primary initiation; Fig. 13 illustrates this, while the proposed approach, based on  $\dot{t}_e$ , is more effective and deterministic.

The  $\tau_s$  values for the Table 2 cases are plotted in Fig. 14, and the corresponding positions on the runway are shown in Fig. 15.

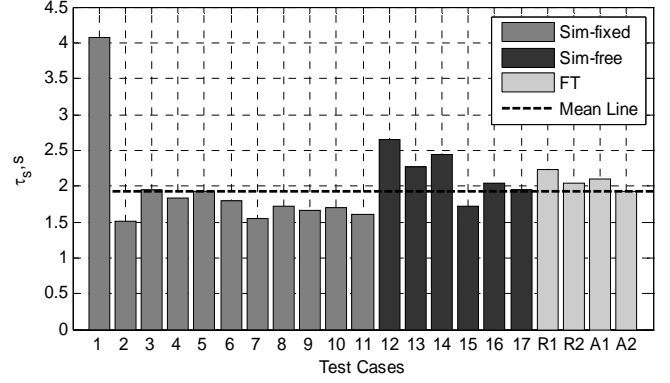


Fig. 14  $\tau_s$  values for initiation of the deceleration phase based on  $\dot{t}_e = 1$

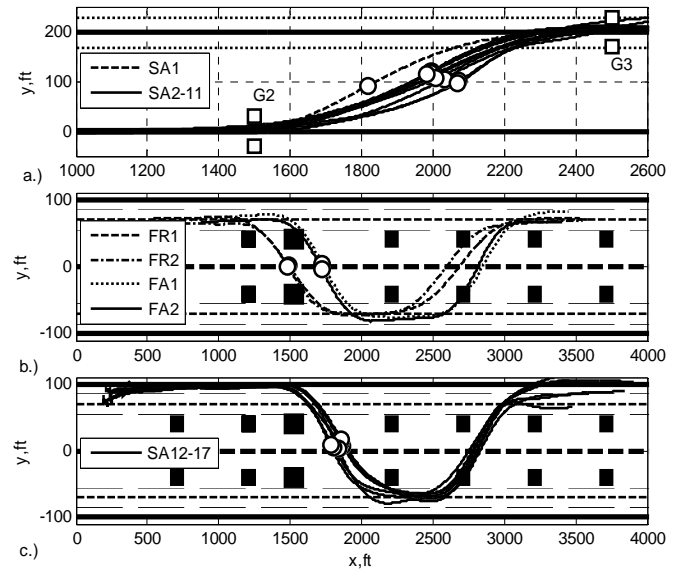


Fig. 15 Corresponding positions in the runway ( $\odot$ ) for the  $\tau_s$  values

Fig. 14 shows that the initiation of the deceleration phase occurs at similar look-ahead  $\tau_s$  values of around 1.5 – 2.5 seconds (excepting case SA1), regardless of the different heights, forward speeds, and pilots; the mean value shown in Fig. 14 is computed without SA1. The timings are consistent with the results from terrain-hugging flight [15]. The initiation points in Fig. 15 are, as expected, located near the centreline; however, as the pilots have indicated, the centreline was not specifically used as a reference to initiate the deceleration.

## B. Determination of $\tau_{bs}$ and $\tau_{be}$

A good deceleration procedure is of critical importance for flying the roll-step with sufficient margin to guide the aircraft through the gates. If  $\dot{t}_e \leq 0.5$ , the lateral movement of the helicopter will stop while aligning with the runway edge. If  $\dot{t}_e > 0.5$ , the helicopter will cross the centreline (the target) and a BAT event with the outer adequate boundary 'may' occur; attention is then focussed on the values of  $\dot{t}_b$  and  $\ddot{t}_b$  at

**Table 3  $\dot{\tau}_b$  and  $\ddot{\tau}_b$  conditions for BAT event and PIOs at the target (edge) crossing**

$\dot{\tau}_b$ Values	$\ddot{\tau}_b$ values	BAT and PIO	Cases
$\dot{\tau}_b < 0.5$	$\ddot{\tau}_b > 0$	BAT event or BAT PIO possible	SA8
	$\ddot{\tau}_b < 0$ but $\ddot{\tau}_b +$	BAT event possible	FA2
	$\ddot{\tau}_b < 0$ but $\ddot{\tau}_b -$	BAT event/PIO unlikely	SA1-7, SA11-17, FR1-2, FA1
$0.5 < \dot{\tau}_b < 1$	$\ddot{\tau}_b > 0$	BAT or C-PIO likely	SA10
	$\ddot{\tau}_b < 0$ but $\ddot{\tau}_b +$	BAT event/PIO likely	SA9
	$\ddot{\tau}_b < 0$ but $\ddot{\tau}_b -$	BAT event likely	
$\dot{\tau}_b > 1$	$\ddot{\tau}_b > 0$	BAT or C-PIO very likely	
	$\ddot{\tau}_b < 0$	BAT or C-PIO likely	

the target crossing, to establish the potential of a BAT event, or, more severely, a BAT PIO. The hypothesised conditions and cases are summarised in Table 3, where C-PIO means conventional PIO.

The conditions have been categorized into three groups according to the value of  $\dot{\tau}_b$ . For the first group with  $\dot{\tau}_b < 0.5$  at the crossing, the lateral movement of a helicopter will normally cease before reaching the boundary. In such cases, the pilot may still choose to change  $\dot{\tau}_b$  in the deceleration phase, reflected in the sign of  $\ddot{\tau}_b$ . In the case of  $\ddot{\tau}_b > 0$  at the crossing,  $\dot{\tau}_b$  increases and consequently the helicopter may overshoot the boundary. The occurrence of a BAT event or BAT PIO then depends on the severity of the related control activity. If  $\ddot{\tau}_b < 0$ , the  $\dot{\tau}_b$  value decreases, but if  $\ddot{\tau}_b$  increases and becomes positive ( $\ddot{\tau}_b +$ ), a BAT event may occur. Due to the reduced severity compared with  $\ddot{\tau}_b > 0$ , the pilot has more time to deal with this situation and a BAT PIO is unlikely. If the variable  $\ddot{\tau}_b$  becomes further negative ( $\ddot{\tau}_b -$ ), no BAT PIO will develop.

The second group involves situations where  $0.5 < \dot{\tau}_b < 1$ , when the helicopter is predicted to reach the boundary with a residual velocity. In this case, there is a strong possibility that a BAT PIO will occur, but three alternative possibilities exist. Firstly, if  $\ddot{\tau}_b > 0$ , the pilot needs to apply more compensatory control and, as a consequence, a conventional PIO or BAT PIO can be triggered. Second, if  $\ddot{\tau}_b < 0$  but  $\ddot{\tau}_b +$ , the approach to the boundary can also be quite aggressive and the BAT PIO is still likely. Finally, if  $\ddot{\tau}_b < 0$  but  $\ddot{\tau}_b -$ ,  $\dot{\tau}_b$  will continue decreasing and the severity will reduce. As a result, a BAT event is likely but a BAT PIO is less likely to occur.

The third group represents the most severe situation, in that the helicopter passes the crossing and approaches the boundary with an acceleration ( $\dot{\tau}_b > 1$ ); then a BAT PIO is usually unavoidable, and its severity depends on the condition of the variable  $\ddot{\tau}_b$ .

The experimental datasets have been categorised by these rules as shown in Table 3. SA8 and FA2 contain BAT events and SA9-10 feature control actuator rate-limiting. For all these cases, there is no consequent BAT PIO as such. For the simulation tests, this is partly because of the large width between the gates, such that the pilot is able to fly through without involving high workload, even for the cases SA9-10. For the cases when the flight speed  $V_x = 100$  kts, larger control inputs are necessary due to the shorter time to cross the runway. As a result, the roll-rate limiter is triggered, resulting in the classic, albeit transient, PIO. For the flight test cases, the period of flying along the  $-70$  ft line is considered to be too short to generate a BAT PIO.

When a BAT event occurs, the  $\tau_{bs}$  value is calculated at the occurrence of the closest peak of  $\ddot{\tau}_b$  at the crossing moment ( $\tau_e = 0$ ). It is hypothesised that the pilot might prefer to take early control action to ensure sufficient safety margin to the boundary. A later response is likely to require a more aggressive control input or lead to the failure of the task. As for the determination of  $\tau_{be}$ , (the end of a BAT event), the approach depends on the situation being investigated. Where the boundary has been crossed, the end of a BAT event is considered as the moment when  $\tau_{be}$  is infinite, or at the furthest distance from the boundary. Under this kind of situation, the pilot will apply a large control input to bring the aircraft back within the boundary. If BAT takes place within the boundary,  $\tau_{be}$  occurs at the moment when  $\dot{\tau}_b$  becomes negative (away from the boundary). Finally,  $\tau_{max}$  is selected in the same way as with Gray's and Warren's approach – the  $\tau_b$  value corresponding to the maximum amplitude of the control input during the BAT PIO.

The two cases SA9 and FA2 are illustrated in Fig. 16 to Fig. 19 to demonstrate the above procedures; the corresponding  $\tau$  values are listed in Table 4 as well as the  $\tau_{bs}$  value (shown as  $\tau_{bsw}$ ) from Warren's method by detecting the sharp increase of stick acceleration [6].

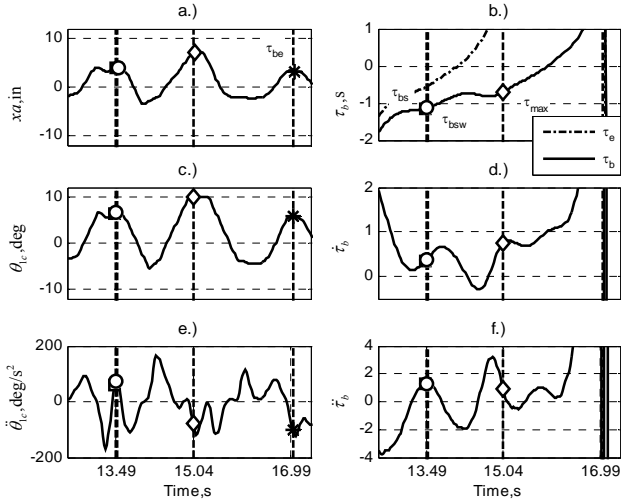


Fig. 16 Selection of BAT parameters from  $\tau$ -theory and Warren's method (SA9)

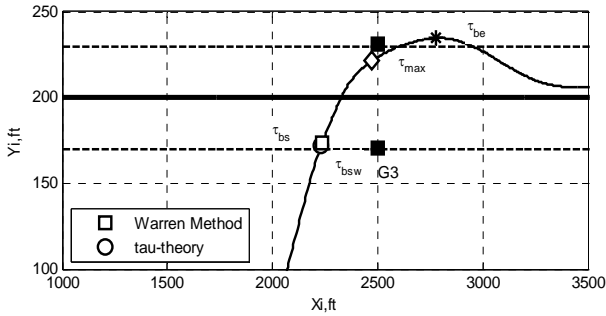


Fig. 17 Related positions of the values selected in Fig. 16 on the runway

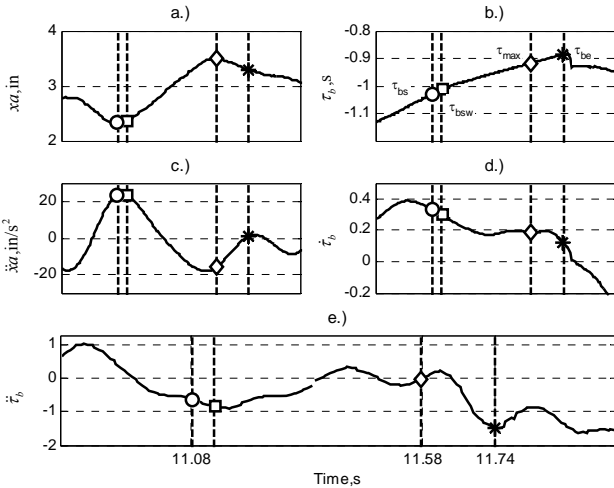


Fig. 18 Selection of BAT parameters from  $\tau$ -theory and Warren's method (FA2)

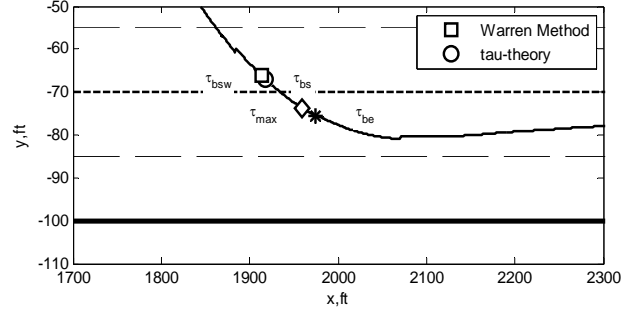


Fig. 19 Related positions of the values selected in Fig. 18 on the runway

Table 4  $\tau_{bs}$  and  $\tau_{be}$  obtained using tau-theory and Warren's method

Method	Proposed		Warren's	
Cases	$\tau_{bs}, S$	$\tau_{be}, S$	$\tau_{bs} - \tau_{max}, S$	$\tau_{bsw} - \tau_{max}, S$
SA8	1.22	1.13	0.29	0.93
SA9	1.16	$\infty$	0.38	0.75
SA10	1.72	$\infty$	1.02	0.28
FA2	1.01	0.89	0.16	0.92

As shown in Fig. 16a for the SA9 case, the lateral input becomes saturated due to the rapid control movement applied to avoid the boundary. The trajectory overshoots the boundary slightly, as shown in Fig. 17. Fig. 16d and Fig. 16e show that both  $\dot{\tau}_b$  and  $\ddot{\tau}_b$  (at  $\tau_e = 0$ ) are at the edge of the critical conditions;  $\dot{\tau}_b$  is larger than 0.5 and  $\ddot{\tau}_b$  is transitioning from  $\ddot{\tau}_b (-)$  to  $\ddot{\tau}_b (+)$ . According to Table 3, there is the potential for a BAT PIO in this case. The consequent rapid control action activated the rate limiter ( $\pm 13$  in/s), shown as the 'sawtooth' shape in Fig. 16a [4], and then a larger control input triggered the input saturation. A Cat II PIO was then a real possibility but the pilot quickly and safely brought the helicopter within the boundaries and the PIO did not materialise due to the large width between the gates. As a result, this situation can be considered as a severe BAT event. The peak of  $\ddot{\tau}_b$  at  $t = 13.49$  seconds determines the  $\tau_{bs}$  value as shown by the line in Fig. 16. After holding the maximum control for a short period, the pilot reduced the input; at  $t = 16.99$  s ( $\tau_b = \infty$ ),  $\tau_{be}$  is selected. Following this, as shown in Fig. 16a, the pilot brought the helicopter back within adequate performance boundary.  $\tau_{bsw}$  is also predicted by Warren's method, as illustrated in Fig. 16a, using the control acceleration (Fig. 16b); the values of  $\tau_{bs}$  and  $\tau_{bsw}$  in Table 4 are seen to be very close.

The same procedure can be applied to the less obvious BAT event in the FA2 case. This BAT event lasts a very short time and stays within the boundary, as shown in Fig. 18 and Fig. 19. Again, very similar values of  $\tau_{bs}$  and  $\tau_{bsw}$  are found, and  $\tau_{be}$  is selected as the point at the peak  $\ddot{\tau}_b$  where  $\dot{\tau}_b$  is continuously reducing. Compared with SA9, more numerical analysis is

required to deal with the flight test data, i.e. filtering and smoothing, and the accuracy of  $\tau_{\text{bsw}}$  degraded.

In addition to the BAT parameters values obtained from tau-theory and Warren's method, Table 4 also reveals differences in  $\tau_b$  between the start of the boundary tracking and the time at the maximum control input. These differences are inconsistent with the fairly constant values ( $0.55 \pm 0.13$  s) predicted by Warren's method [6]. Warren considered this value as an intrinsic human characteristic. However, variation of this value is possible and physically reasonable, as shown by the cases above. This is partly because  $\tau_b$  is distinct from the manoeuvre time  $T$ .  $\tau_b$  and the control input may not vary smoothly during a BAT event but rather evolve nonlinearly, as shown in the SA9 and FA2 cases. This emphasises that a nonlinear feedback loop is required for modelling the BAT event, a characteristic of tau guide following.

The BAT parameter predictions from tau-theory provide a glimpse of the power of using the optical variables, rather than trajectory or control variables to define the propensity to PIOs. At this point in the development of the theory we have shown application to predicting the critical  $\tau_b$  parameters. The continuing research is exploring the even more attractive prospect of predicting situations of incipient PIOs ahead of the  $\tau_b$  crossing, based on the  $\Delta\tau$  between target and boundary, providing the information needed to create a PIO alert system. The success of this approach depends on robust and rapid sensing of  $\tau$  and  $\dot{\tau}$ , a research area in its own right.

## VI. CONCLUSIONS

The research presented in this paper has brought together optical tau theory and boundary-avoidance tracking developments in flight control. Preliminary results from flight and simulator testing with a roll-step boundary tracking manoeuvre have been analysed from the two different perspectives. The main conclusions derived from the present study are as follows:

- 1.) Roll step control can be modelled as a prospective strategy by coupling lateral motion onto an intrinsic tau guide to fly the runway acquisition and tracking. The guide takes the constant deceleration form, such that  $\dot{\tau}$  is a constant throughout the deceleration phase. With  $\dot{\tau} < 0.5$  maintained during the deceleration, the pilot is assured of a successful outcome to the MTE.
- 2.) The  $\dot{\tau}_e = 1$  point has been shown to predict the initiation of the deceleration of the roll-step manoeuvre. The present study has shown that the pilot attempts to start decelerating when the time to the runway edge,  $\tau_e$ , is around two seconds regardless of the initial forward speed and height in both simulator and flight tests.
- 3.) Deviations from the  $\dot{\tau}$  constant strategy are manifest in variations in  $\ddot{\tau}$  and this has been exploited in the present study as a basis for determining the BAT timing parameters, in contrast to the control acceleration variations in the Gray-Warren model.

- 4.) Tau theory has provided an effective and feasible approach to determining the start and end BAT parameters  $\tau_{bs}$  and  $\tau_{be}$ . The results show good agreement with Warren's method but also provide a general framework for classifying the likely outcome based on values of  $\tau$ ,  $\dot{\tau}$  and  $\ddot{\tau}$  at the edge crossing point, hence distinguishing between a successful tracking, a BAT event and the PIOs.

Further experiments are required to validate fully the approach proposed in this paper and extend to other aircraft types and manoeuvres. For example, aircraft more prone to experience fully developed PIO cases should be investigated, when the efficacy of early warning systems based on the direct measurement of tau and its derivatives can be explored.

## ACKNOWLEDGMENTS

The research reported in this paper was funded by the UK Engineering and Physical Sciences Research Council grants EP/D003512/1 (Rotorcraft-Pilot Couplings) and EP/G002932/1 (Lifting Standards). Special thanks go to test pilot Andy Berryman for his valuable contributions to the project and to Philip Perfect, for his dedicated support in dealing with the raw flight test data. The flight test data was supplied through collaboration with the NRC Ottawa, Flight Research Laboratory, and the NRC staff support is greatly appreciated.

## REFERENCES

- [1] Padfield, G. D., *Helicopter Flight Dynamics*, 2<sup>nd</sup> ed., Blackwell Science, Oxford, 2007.
- [2] Pavel, M. D., and Padfield, G. D., "Understanding the Peculiarities of Rotorcraft-Pilot Couplings," *64<sup>th</sup> Annual Forum of the American Helicopter Society*, Montreal, Canada, May 2008.
- [3] Lu, L., Padfield, G. D., and Jump, M., "The Strongly Controlled Helicopter", *34<sup>th</sup> European Rotorcraft Forum*, Liverpool, UK, 16 – 19 Sept. 2008.
- [4] McRuer, D. T., et al., *Aviation Safety and Pilot Control Understanding and Preventing Unfavourable Pilot-Vehicle Interactions*, National Academy Press, ASEP National Research Council, Washington D.C., 1997.
- [5] Gray III, W. R., "Boundary-Avoidance Tracking: A New Pilot Tracking Model," *AIAA Atmospheric Flight Mechanics Conference and Exhibit*, San Francisco, California, 15 - 18 Aug., 2005, pp. 86-97.
- [6] Warren, R. D., "An Investigation of the Effects of Boundary Avoidance on Pilot Tracking," MSc Thesis, Department of the Air Force Air University, United States Air Force Institute of Technology, Wright-Patterson Air Force Base, Ohio, 2006.
- [7] Warren, R. D., Abell, B., Heritsch, S., Kolsti, K., and Miller, B., "Limited Investigation and Characterization of

- Boundary Avoidance Tracking (Project HAVE BAT)," Air Force Flight Test Center Edwards AFB CA, June 2006.
- [8] Pavel, M.D., et al., Adverse Rotorcraft-Pilot Couplings – Prediction and Suppression of Rigid Body RPCs, proc. 34<sup>th</sup> European Rotorcraft Forum, Liverpool, England, September 16-18<sup>th</sup> 2008
- [9] Lee, D. N., "Guiding Movement by Coupling Taus," *Ecological Psychology*, Vol. 10, No. 3, 1998, pp. 221-250.
- [10] Gibson, J. J., "The Perception of the Visual World," *AJP*, Vol. 64, 1951, pp. 622-625.
- [11] Lee, D. N., Craig, C. M., and Grealy, M. A., "Sensory and Intrinsic Coordination of Movement," *Proc. of Biological sciences*, Vol. 266, No. 1432, Jul.1999, pp. 2029-2035.
- [12] Lee, D. N., "Tau in Action in Development," *Action as an Organizer of Learning and Development*, edited by. J. J. Rieser, J. J. Lockman, and C. A. Nelson, 33rd Volume in the Minnesota Symposium on Child Psychology, Minnesota, 2005, pp. 3-50.
- [13] Lee, D. N., "How movement is guided," Psychology Department, School of Philosophy, Psychology and Language Sciences, University of Edinburgh, 2006.
- [14] Padfield, G. D., Lee, D. N., and Bradley, R., "How Do Helicopter Pilots Know When to Stop, Turn or Pull Up?," *AHS Journal*, Vol. 48, No. 2, 2003, pp. 108-119.
- [15] Padfield, G. D., Clark, G., and Taghizad, A., "How Long Do Pilots Look Forward? Prospective Visual Guidance in Terrain-Hugging Flight," *AHS Journal*, Vol. 52, No. 2, 2007, pp. 134-145.
- [16] Jump, M., and Padfield, G. D., "Investigation of the Flare Manoeuvre Using Optical Tau," *J Guid Contr Dynam*, Vol. 29, No. 5, pp. 1189-1200, Sept.2006.
- [17] Jump, M., and Padfield, G. D., "Progress in the Development of Guidance Strategies For the Landing Flare Manoeuvre Using Tau-based Parameters," *Aircraft Eng Aero Tech*, Vol. 78, No. 1, 2006, pp. 4-12.
- [18] Clark, G., "Helicopter Handling Qualities in Degraded Visual Environments (DVE)," Department of Engineering, The University of Liverpool, UK, 2007.
- [19] Meyer, M., and Padfield, G. D., "First Steps in the Development of Handling Qualities Criteria for a Civil Tilt Rotor," *AHS Journal*, Vol. 50, No. 1, 2005, pp.33-46.
- [20] Anon., *Aeronautical Design Standard Performance Specification Handling Qualities Requirements for Military Rotorcraft ADS-33E-PRF*, US Army Aviation and Missile Command, Aviation Engineering Directorate, Redstone Arsenal, Alabama, Mar. 2000.
- [21] Hess, R. A., "Unified Theory for Aircraft Handling Qualities and Adverse Aircraft–Pilot Coupling," *J Guid Contr Dynam*, Vol. 20, No. 6, pp. 1141-1148, Nov.1997.
- [22] Lee, D. N., "A Theory of Visual Control of Braking Based on Information about Time-To-Collision," *Perception*, Vol. 5, No. 4, 1976, pp. 437-459.
- [23] Padfield, G. D., and White, M. D., "Flight Simulation in Academia; HELIFLIGHT in Its First Year of Operation," *Aeronaut J*, Vol. 107, No. 1075, Sept. 2003, pp. 529-538.
- [24] White, M. D., Padfield, G.D., Perfect, P., Gubbels, A. W. and Berryman, A. C., "Acceptance Testing of A Rotorcraft Flight Simulator for Research and Teaching: the Importance of Unified Metrics," Proc. of the 35th European Rotorcraft Forum, Hamburg, Germany, Sept. 2009.
- [25] Manimala, B., Walker, D., and Padfield, G. D., "Rotorcraft Simulation Modelling and Validation for Control Law Design," *Aeronaut J*, Vol. 111, Feb.2007, pp. 77-88.
- [26] Kaiser, M. K., "Optical Specification of Time-to-Passage: Observers' Sensitivity to Global Tau," *Journal of Experimental Psychology: Human Perception and Performance*, Vol. 19, No. 5, 1993, pp. 1024-1040.
- [27] Lee, D. N., and Reddish, P. E., "Plummeting Gannets: a Paradigm of Ecological Optics," *Nature*, Vol. 293, Sept. 1981, pp. 293-294.

**APPENDIX A - DERIVATION OF TAU-GUIDE FOLLOWING MOTION FORMS**

Constant Deceleration Guide	Constant Velocity Guide	Constant Acceleration Guide
<i>g motion</i>		
$a_g = a_{g0}$ $v_g = v_{g0} + a_{g0} t$ $x_g = x_{g0} + v_{g0} t + \frac{a_{g0}}{2} t^2$ $x_g = x_{g0}(1-\hat{t})^2$ $v_g = -\frac{2x_{g0}}{T}(1-\hat{t})$ $v_{g0} = -\frac{2x_{g0}}{T} \quad a_{g0} = \frac{2x_{g0}}{T^2}$ $\tau_g = -\frac{1}{2}(T-t) = \frac{1}{2}(2\tau_{g0}+t)$ $\hat{t}_g = -\frac{1}{2}(1-\hat{t})$ $\dot{t}_g = \dot{\hat{t}}_g = 1$	$a_g = 0$ $v_g = v_{g0}$ $x_g = x_{g0} + v_{g0} t$ $x_g = x_{g0}(1-\hat{t})$ $v_g = v_{g0}$ $v_{g0} = -\frac{x_{g0}}{T} \quad a_{g0} = 0$ $\tau_g = t - T = t + \tau_{g0}$ $\hat{t}_g = -(1-\hat{t})$ $\dot{t}_g = \dot{\hat{t}}_g = 1$	$a_g = a_{g0}$ $v_g = v_{g0} + a_{g0} t$ $x_g = x_{g0} + v_{g0} t + \frac{a_{g0}}{2} t^2$ $x_g = x_{g0}\left(1 + \frac{Tv_{g0}}{x_{g0}}\hat{t} - \left(1 + \frac{Tv_{g0}}{x_{g0}}\right)\hat{t}^2\right)$ $v_g = v_{g0} - \frac{2x_{g0}}{T}\left(1 + \frac{Tv_{g0}}{x_{g0}}\right)\hat{t}$ $v_{g0} = 0$ $a_{g0} = -\frac{2x_{g0}}{T^2}\left(1 + \frac{Tv_{g0}}{x_{g0}}\right)$ $x_g = x_{g0}(1-\hat{t}^2) \quad v_g = -\frac{2x_{g0}}{T}\hat{t}$ $\tau_g = -\frac{T}{2}\left(\frac{1}{\hat{t}} - \hat{t}\right)$ $\hat{t}_g = -\frac{1}{2}\left(\frac{1}{\hat{t}} - \hat{t}\right)$ $\dot{t}_g = \dot{\hat{t}}_g = \frac{1}{2}\left(1 + \frac{1}{\hat{t}^2}\right)$
<i>y motion</i>		
$\tau_y = k \tau_g \quad y = C x_g^{1/k}$		
$\hat{y} = -(1-\hat{t})^{2/k}$ $\hat{y} = \frac{2}{k}(1-\hat{t})^{\left(\frac{2}{k}-1\right)}$ $\hat{y} = -\frac{2}{k}\left(\frac{2}{k}-1\right)(1-\hat{t})^{2\left(\frac{1}{k}-1\right)}$ $\hat{t}_y = -\frac{k}{2}(1-\hat{t})$ $\dot{\hat{t}}_y = \dot{\tau}_y = \frac{k}{2}$ $T = -\frac{2\tau_{y0}}{k}$	$\hat{y} = -(1-\hat{t})^{1/k}$ $\hat{y} = \frac{1}{k}(1-\hat{t})^{\left(\frac{1}{k}-1\right)}$ $\hat{y} = -\frac{1}{k}\left(\frac{1}{k}-1\right)(1-\hat{t})^{\left(\frac{1}{k}-2\right)}$ $\hat{t}_y = -k(1-\hat{t})$ $\dot{\hat{t}}_y = \dot{\tau}_y = k$ $T = -\frac{\tau_{y0}}{k}$	$\hat{y} = -(1-\hat{t}^2)^{1/k}$ $\hat{y} = \frac{2\hat{t}}{k}(1-\hat{t}^2)^{\left(\frac{1}{k}-1\right)}$ $\hat{y} = -\frac{2}{k}\left(\left(\frac{2}{k}-1\right)\hat{t}^2 - 1\right)(1-\hat{t}^2)^{\left(\frac{1}{k}-2\right)}$ $\hat{t}_y = -\frac{k}{2}\left(\hat{t} - \left(\frac{1}{\hat{t}}\right)\right)$ $\dot{\hat{t}}_y = \frac{k}{2}\left(1 + \left(\frac{1}{\hat{t}}\right)^2\right)$

## APPENDIX B

If two motion gaps  $x$  and  $y$  are coupled with a constant  $k$ , then their coupling relationship can be described as follows,

$$\tau_y = k\tau_x \quad \text{B(1)}$$

then the motion gap  $y$  can be given by

$$y = C(-x)^{1/k} \quad \text{B(2)}$$

where  $C$  is a constant. Thus

$$\dot{y} = C(1/k)(-x)^{1/k-1}(-\dot{x}) \quad \text{B(3)}$$

$$\ddot{y} = C(1/k)(-x)^{1/k-2}[(1/k-1)\dot{x}^2 - x\ddot{x}] \quad \text{B(4)}$$

Taking into account what happens when  $x \rightarrow -0$ :

- a.) If  $k < 0$ , then  $y \rightarrow -\infty$ ,  $\dot{y} \rightarrow +\infty$ , and  $\ddot{y} \rightarrow \infty$ . This case has no physical meaning.
- b.) If  $0 < k \leq 0.5$ , then  $y \rightarrow -0$ ,  $\dot{y} \rightarrow +0$ , and  $\ddot{y} \rightarrow \pm 0$ . The motion  $y$  will stop before the obstacle.
- c.) If  $0.5 < k < 1$ , then  $y \rightarrow -0$ ,  $\dot{y} \rightarrow +0$ , and  $\ddot{y} \rightarrow \pm 0$ . The motion  $y$  will stop before the obstacle.
- d.) If  $k = 1$ , then  $y \rightarrow -0$ ,  $\dot{y} \rightarrow +0$ , and  $\ddot{y} \rightarrow -C_1$  (constant). This means that the motion  $y$  will just stop at the obstacle with residual deceleration.
- e.)  $1 < k < 2$ , then  $y \rightarrow -0$ ,  $\dot{y} \rightarrow +C_2$  (constant) and  $\ddot{y} \rightarrow -\infty$ . This means that the motion  $y$  will contact the obstacle with an infinite deceleration.
- f.)  $k = 2$ , then  $y \rightarrow -0$ ,  $\dot{y} \rightarrow +C_3$  (constant) and  $\ddot{y} \rightarrow \pm 0$ . This means that the motion  $y$  will contact the obstacle with residual velocity.
- g.)  $k > 2$ , then  $y \rightarrow -0$ ,  $\dot{y} \rightarrow +\infty$ , and  $\ddot{y} \rightarrow +\infty$ . This means that the motion  $y$  will accelerate toward the obstacle.

### Proof for Condition C:

Because  $0.5 < k < 1$ , then  $0 < (1/k) - 1 < 1$  and  $-1 < (1/k) - 2 < 0$ . Thus when  $x \rightarrow -0$ ,  $\dot{y} \rightarrow +0$ .

$$\begin{aligned} \lim_{x \rightarrow -0} \ddot{y} &= \lim_{x \rightarrow -0} \{C(1/k)(-x)^{1/k-2}[(1/k-1)\dot{x}^2 - x\ddot{x}]\} \\ &= C(1/k) \lim_{x \rightarrow -0} \{(-x)^{1/k-2}[(1/k-1)\dot{x}^2 - x\ddot{x}]\} \\ &= C(1/k)(1/k-1) \lim_{x \rightarrow -0} [(-x)^{1/k-2}\dot{x}^2] - C(1/k) \lim_{x \rightarrow -0} [(-x)^{1/k-1}\ddot{x}] \end{aligned} \quad \text{B(5)}$$

For the intrinsic constant deceleration guidance,  $\ddot{x} = g$ . Therefore, the second term in Eq. B(5) is zero; as for the first term in Eq. B(5),

$$\begin{aligned} \lim_{x \rightarrow -0} [(-x)^{1/k-2}\dot{x}^2] &= \lim_{x \rightarrow -0} \frac{\dot{x}^2}{(-x)^{2-1/k}} = \lim_{x \rightarrow -0} \frac{2\dot{x}\ddot{x}}{(2-1/k)(-x)^{1-1/k}(-\dot{x})} \\ &= \lim_{x \rightarrow -0} \frac{-2g}{(2-1/k)(-x)^{1-1/k}} = \frac{-2g}{(2-1/k)} \lim_{x \rightarrow -0} (-x)^{1/k-1} \\ &= 0 \end{aligned} \quad \text{B(6)}$$